



Development of a versatile rotating ring-disc electrode for *in situ* pH measurements



Alexsandro Mendes Zimer^a, Marina Medina da Silva^a, Eduardo G. Machado^b, Hamilton Varela^b, Lucia Helena Mascaro^a, Ernesto Chaves Pereira^{a,*}

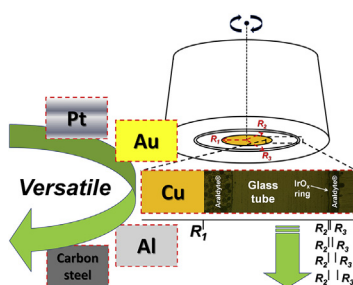
^a Laboratório Interdisciplinar de Eletroquímica e Cerâmica (LIEC), Federal University of São Carlos (UFSCar), Chemistry Dept., PO Box: 676, CEP: 13.565-905, São Carlos, SP, Brazil

^b Institute of Chemistry of São Carlos, University of São Paulo (USP), PO Box: 780, CEP: 13560-970, São Carlos, SP, Brazil

HIGHLIGHTS

- A rotating ring/disc electrode using as ring IrO_x to sense pH was built.
- The electrode showed fast response during pH transients.
- The system is versatile and as disc any material can be used.
- The system can be polished without the destruction of the disc and ring sensor materials.

GRAPHICAL ABSTRACT



ARTICLE INFO

Article history:

Received 25 April 2015

Received in revised form

29 September 2015

Accepted 30 September 2015

Available online 8 October 2015

Keywords:

Interfacial pH measurements

Iridium oxide

Rotating ring-disc electrode

Ultramicroelectrode

ABSTRACT

There are some electrocatalytic reactions in which the key parameter explaining their behavior is a local change in pH. Therefore, it is of utter importance to develop an electrode that could quantify this parameter *in situ*, but also be customizable to be used in different systems. The purpose of this work is to build a versatile rotating ring/disc electrode (RRDE) with IrO_x deposited on a glass tube as a ring and any kind of material as disc. As the IrO_x is sensitive to pH variation, the reactions promoted on the disc can trigger proportional pH shifts on the ring. In such assembly, the IrO_x ring presents a fast response time even during the pH transients due to the small thickness of the ring (approximately 10 μm), which enables the detection of interfacial pH changes. The ring electrode was tested toward the interfacial pH shift observed during the electrolytic reduction of water on the disc and also characterized by acid–base titration to determine the response time. As the main conclusions, fast response and durable RRDE were obtained, and this assembly could be used to revisit many electrocatalytic reactions in order to test the importance of local pH on the process.

© 2015 Elsevier B.V. All rights reserved.

1. Introduction

Interfacial pH measurements are important to explain anomalous behavior observed in different electrochemical systems.

Indeed, pH changes can be the key issue in many interfacial processes, which can be only explained by a local pH transient variation at the electrode/solution interface [1–6]. For example, the electrodeposition of Co could lead to the formation of Co(OH)₂ even when the bulk solution is acidic [1,2]. To explain this phenomenon, the authors considered the water reduction which leads to hydrogen evolution, and, as a consequence, to the formation of

* Corresponding author.

E-mail address: lmascaro@ufscar.br (L.H. Mascaro).

hydroxide ions causing the precipitation of $\text{Co}(\text{OH})_2$. Nobial et al. [4] has also described the production of OH^- ions at the electrode surface, thus increasing the local pH to promote the precipitation of metallic oxide/hydroxide on the surface. In the anomalous electrodeposition of Ni–Fe alloys [5], the electrochemically less noble metal deposits preferentially on the surface of more noble metal [5], and this phenomenon could be explained by an interfacial pH transient. Nakano et al. [6] proposed that this phenomenon depends on the pH buffer capacity of the solution and, via a multi-step reduction process, FeOH adsorbs preferentially over the nucleation sites of nobler metal due to the extremely lower dissociation constant of iron and nickel hydroxides [6]. This process occurs only because the chemical equilibrium and reaction kinetics are rather different from the bulk solution due to the different pH values near the surface.

The measurement of the transient pH shift caused by an electrochemical reaction is a difficult task. Desloius et al. [7], using a sensor–grid assembly, detected interfacial pH changes during the reduction of dissolved oxygen using an impinging jet cell that needs high controlled flow to measure the pH change near the surface. *In situ* pH measurements from different systems are widely described in the literature using microelectrode devices [8,9] or AFM tips [10,11]. Microelectrodes can also be used for *in vivo* determinations of pH [12], but in some cases, the application of interfacial pH measurements is difficult to perform using these microdevices because of the dynamic chemical state of this reaction. On the other hand, rotating ring/disc electrodes (RRDEs) are devices developed to investigate dynamic processes on surfaces allowing the control of the flow of species to the ring by setting a suitable rotating rate [13,14]. In this method, the steady state is attained quickly, which increases the precision of the measurement [15]. A conventional RRDE, with the disc and the ring made of Pt, has been largely used to perform current and potential analysis [15,16]. In the latter, the disc is polarized at a constant potential to promote a specific reaction while the current–potential curves are collected on the ring [15,16]. The convective–diffusion equations to RRDE were presented by Albery and Bruckenstein [17] using a proper choice of adequate boundary conditions. The authors also described the collection efficiency (N) of this kind of electrode (Eq. (1) and Eq. (2)), which is defined as a percentage of the product generated at the disc that is collected at the ring [15].

$$N = \left(1 - F[\alpha/\beta] + \beta^{2/3}(1 - F[\alpha]) - (1 + \alpha + \beta)^{2/3} \right. \\ \left. \times (1 - F[(\alpha/\beta)(1 + \alpha + \beta)]) \right) \quad (1)$$

where $\alpha = (R_2/R_1)^3 - 1$, $\beta = (R_3/R_1)^3 - (R_2/R_1)^3$, R_1 is the radius of disc electrode, R_2 and R_3 are the inner and outer radius of ring electrode, respectively, and the F values are calculated according to Eq. (2).

$$F[\theta] = \frac{3^{1/2}}{4\pi} \text{Ln} \left[\frac{(1 + \theta^{1/2})^3}{1 + \theta} \right] + \frac{3}{2\pi} \text{ArcTan} \left[\frac{(2\theta^{1/3} - 1)}{3^{1/2}} \right] + \frac{1}{4} \quad (2)$$

Besides collecting and shielding experiments [15,16], the ring could be used as a potentiometric sensor for pH measurements [13], as proposed by Albery and Calvo. In this system, the ring electrode was prepared by room-temperature electroplating, and it was used as a potentiometric detector for pH. In that paper, an equivalent term to N was introduced, the detection efficiency (N_D), which compares the changes in pH at the ring electrode with those on the disc surface [13]. N_D is defined by (Eq. (3)) below [13].

$$N_D = 1 - 1/6F \left[(R_2/R_1)^3 - 1 \right] - 2/3F \left[((R_2 + R_3)/2R_1)^3 - 1 \right] \\ - 1/6F \left[(R_3/R_1)^3 - 1 \right] \quad (3)$$

Some promising materials to prepare pH devices are the metal oxides [18], and among them, the iridium oxide electrodes are in the spotlight because of their stability and high sensitivity [9]. IrO_x is a metallic conductor sensitive to pH variations [8,19] because it can exist on a variety of oxidation states [20]. In that sense, this material allows us to make a pH sensor in different shapes and sizes using an adequate synthesis method: polymeric precursor method (Pechini) [8] or anodic electrodeposition [21]. In the latter, the oxide film is produced only on conductive materials, while in the Pechini method, different types of substrates, or even non-conductive materials, can be employed [8].

In this work, we describe the fabrication and characterization of a RRDE for interfacial pH measurements. The ring consists of a thin film of IrO_x synthesized by the Pechini method [8] on a glass tube. The tube thickness is the gap between the ring and the disc. Then, the ring is used as a potentiometric detector of the ring/solution interface. As the iridium oxide is a pH sensor, the ring potential is influenced by the species formed on the disc that are continuously swept from it to the ring by convection due to the electrode rotation. Therefore, by means of a calibration curve, it is possible to calculate the values of interfacial changes of pH on the disc.

2. Experimental section

2.1. Construction of the RRDE to pH measurements

To build the RRDE ($\text{IrO}_x/\text{Metal}$), the pH sensitive layer of IrO_x was deposited using the polymeric precursor method (Pechini), following the procedure previous described in literature [8], on a boron silicate glass tube with outer and inner diameters of 7 mm and 5 mm, respectively. The flowchart of this procedure is shown in Fig. 1. First, the glass substrate was sandblasted and then treated in boiling concentrated HCl. Finally, the glass tube was washed with purified water (Gehaka model OS20 LX FARMA) and dried under N_2 flow. The polymeric precursor was generated by dissociation of citric acid (CA) in ethylene glycol (EG) at 65 °C under stirring. Then, the IrCl_3 was added to the mixture using a molar ratio of 0.5:3:12 (IrCl_3 :CA:EG) [8]. Aliquots of 25 μL of this solution were dripped on the outside of a glass tube and then distributed uniformly using a small brush within a length of 2 cm (see inset (a) of Fig. 1). During this step, the glass tube was kept under rotation (see inset (a) of Fig. 1) and on hot air flow to uniformly distribute the resin. Then, a sequential calcination was performed at temperatures of 130, 250, and 400 °C during 30, 20, and 10 min, respectively, to generate IrO_x film [19]. The inset (b) of Fig. 1 shows some glass tubes after the calcination steps. This procedure was repeated four times to increase the thickness of the oxide. After these steps, a copper rod was inserted into the glass tube and sealed using Araldite® (see inset (c) of Fig. 1). The metal disc in the center of the electrode has an area (A_{disc}) of 0.181 cm^2 . It is important to stress that any kind of noble or non-noble metal can be used as disc. This possibility makes the sensor a versatile setup which can be applied to the study of different systems. The electrical contacts were made with conductive silver ink between the external part of the glass tube and a copper wire (see inset (c) of Fig. 1). Finally, the system was sealed with Araldite® and polyester resin to form the outside part of the RRDE pH sensor (see inset (d) of Fig. 1). The disc and ring contacts were positioned according to the commercial rotation system employed in this work, Fig. 1.

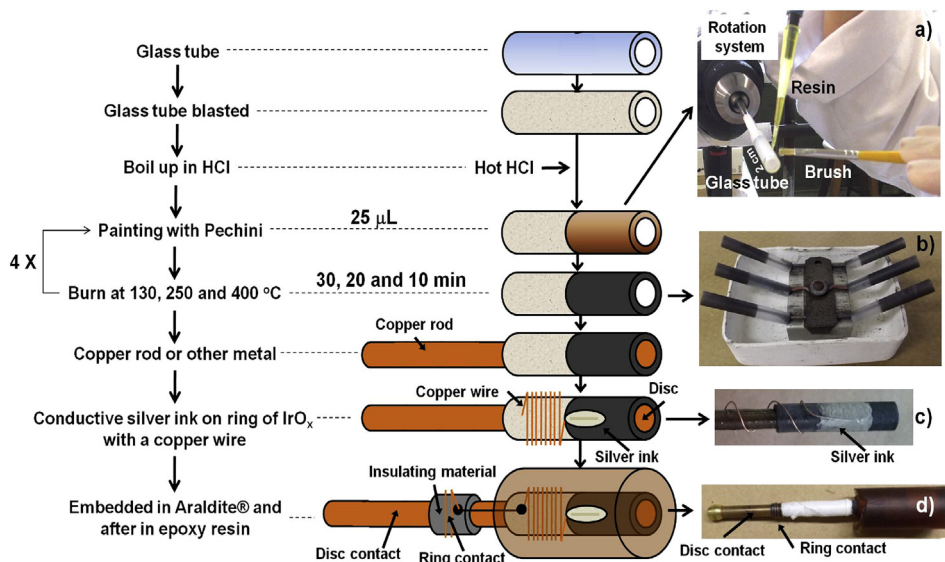


Fig. 1. Flowchart describing the experimental procedure for assembly of versatile RRDE pH sensor ($\text{IrO}_x/\text{Metal}$). $A_{\text{disc}} = 0.181 \text{ cm}^2$. Insets: painting with the Pechini resin (a); calcination (b); ring contact (c); and final electrode (d).

2.2. Equipments

A rotation system EG&G PARC, model 636, coupled to a Bipotentiostat Autolab PGSTAT 30 controlled by NOVA 1.6 software was used to measure the $E_{\text{IrO}_x, \text{ring}}$ at the ring while the copper disc was used as reference electrode (RE). A circular Pt sheet was used as counter electrode (CE) and the RRDE as working electrode 1 and 2 (WE_1 and WE_2).

The ring thickness was measured by observing the RRDE surface using an inverted optical microscope (Opton, mod. TNM-PL-07T).

A pH meter (Denver, Ultrabasic, mod. UB-10) and a Fluka 8085A digital multimeter were used in the initial characterization of the IrO_x ring. These pH experiments were followed simultaneously with a combined glass electrode module CW711X/Qualxtrom to compare to the IrO_x ring electrode performance.

2.3. Procedure

Prior to use, the RRDE was abraded with sandpaper from 320 up to 1200 grit and then polished with alumina ($0.3 \mu\text{m}$). Next, the electrode was washed in deionized water for 60 s in an ultrasonic bath. It is important to note that the RRDE pH sensor used in this work allowed the abrading of the disc surface without interfering with the response of the ring pH sensor. However, the use of sandpaper below 320 grit is discouraged to avoid breaking the glass ring.

The N and N_D were determined geometrically according to the literature [13,17] from the dimensions of the electrode (Eqs. (1)–(3)).

The calibration of ring pH sensor was performed by titration curves of NaOH 0.1 mol L^{-1} (Quimis) with H_3PO_4 1.0 mol L^{-1} (Mallinckodt) with the electrode in the stationary mode and in rotating mode where just the $E_{\text{IrO}_x, \text{ring}}$ was collected every 0.5 s or 0.1 s, respectively, during the titrations. The rotation rates used were 300, 600, 900, 1200, 1500, and 1800 rpm [15]. These results are shown in the two first subsections of the Results and Discussion section.

After the ring performance test, a new experiment was carried out. In such an experiment, the pH shift was due to a specific reaction performed on the disc that produced an interfacial pH change. The reaction chosen to test the RRDE pH sensor ($\text{IrO}_x/\text{Metal}$) was the water reduction. Then, the disc was cathodically polarized in a deaerated solution of $0.1 \text{ mol L}^{-1} \text{Na}_2\text{SO}_4$ (JTBaker) at approximately pH 6.5, prepared with boiled distilled water. Disc chronoamperometric measurements (CAs) were performed at potentials of -0.5 , -0.75 , and -1.0 V while the $E_{\text{IrO}_x, \text{ring}}$ was used to monitor the interfacial pH by changes in the open circuit potential value. In this step, a new calibration curve was made using the same solution by titration of $0.1 \text{ mol L}^{-1} \text{Na}_2\text{SO}_4$ (JTBaker) with NaOH 0.1 mol L^{-1} (Quimis). These results are shown in the last subsection of Section 3.

3. Results and discussion

3.1. Characterization of the RRDE

Fig. 2 shows a schematic representation of RRDE with their respective radii: R_1 , R_2 , and R_3 as described before. The gap between the disc and the ring ($R_2 - R_1$) was $1210 \mu\text{m}$. Due to this large gap, the influence of the disc current over the ring process is negligible, as proposed by Miksis and Newman [22]. The thickness of the pH sensor ring ($R_3 - R_2$) was about $9.9 \pm 3.7 \mu\text{m}$, according the optical microscopy of its surface (Fig. 2 inset). Considering its dimension, the disc of the RRDE described here is an ultramicroelectrode (UME) [23] for interfacial pH measurements [23].

Using the image presented in Fig. 2, the geometrical parameters were measured: $R_1 = 0.240 \text{ cm}$, $R_2 = 0.361 \text{ cm}$, and $R_3 = 0.362 \text{ cm}$. N and N_D were determined geometrically according to the literature [13,17] as 1.9%, and 20%, respectively (Eqs. (1)–(3)). For pH measurements, N_D is the most important parameter because it is the percentage of species that are generated on the disc which are collected on the ring, causing interfacial pH shifts [13]. This value is very close to that found in the literature by Albery and Calvo [13] for the geometry used in that work (N_D 26.2%).

Due to the large gap between the ring and disc, the influence of the disc current over the ring process is negligible using this

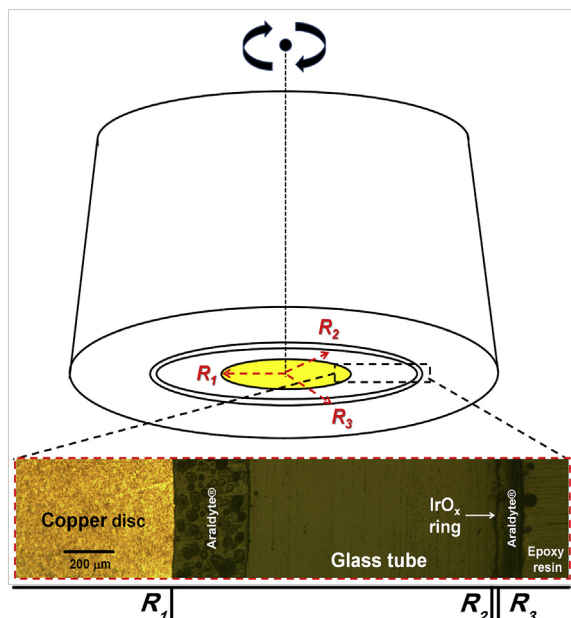


Fig. 2. Schematic representation of the versatile RRDE pH sensor. Radius of the copper disc (R_1), inner (R_2) radius, and outer (R_3) radius of IrO_x ring electrode. Optical microscopy of IrO_x ring (pH sensor) around of the copper disc (Inset).

geometry, as proposed by Miksis and Newman [22].

3.2. Test of the RRDE performance for pH measurements in stationary mode

Initially, acid–base titrations were performed with the electrode in the stationary mode to characterize the RRDE pH sensor for significant pH shifts on the bulk of the solution. Fig. 3a shows the titration of 0.1 mol L^{-1} NaOH with 1.0 mol L^{-1} H_3PO_4 together with the pH measurement obtained through a combined glass electrode (see arrows in Fig. 3a). The variation of $E_{\text{IrO}_x, \text{ring}}$ of the RRDE pH sensor was very close to the pH determined by the conventional glass sensor displaying the same profile for the first and second dissociation constants. Another important point to stress is that the IrO_x deposited over the glass tube remained sensitive to pH measurements even when supported on a non-conductive material, such as the glass tube, considering the small thickness of the oxide film.

The graph of $E_{\text{IrO}_x, \text{ring}}$ as a function of the pH is shown in Fig. 3b

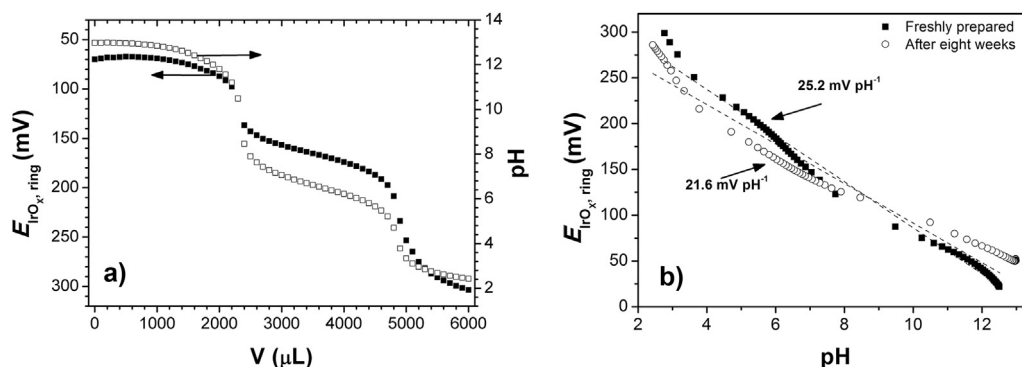


Fig. 3. Titration curve of NaOH (0.1 mol L^{-1}) titrated with H_3PO_4 (1 mol L^{-1}) with the RRDE in stationary mode (a), where (■) is the $E_{\text{IrO}_x, \text{ring}}$ and (□) is the pH observed at pH meter both as function of the volume of titrant added. Calibration curve to $E_{\text{IrO}_x, \text{ring}}$ as a function of the pH for a freshly prepared electrode and after eighth weeks of aging (b). $E_{\text{IrO}_x, \text{ring}}$ collected every 0.5 s during titration.

for a freshly prepared electrode and for an aged electrode (eight weeks later). The $E_{\text{IrO}_x, \text{ring}}$ observed over the range of pH from 12.5 to 2.5 showed linear behavior in both cases. It is important to note that $E_{\text{IrO}_x, \text{ring}}$ ranged approximately 250 mV between the two extremes of the titration, pH 12.5–pH 2.5, which highlights its sensitivity to pH shifts in the solution. The linear band has an average pH gradient of $23 \pm 4 \text{ mV pH}^{-1}$ calculated from triplicate electrodes. The sub-Nernstian behavior for the UME pH sensor could be explained by the absence of conductive substrate under the active oxide, once it was observed in previous studies a slope of $56.9 \pm 0.2 \text{ mV pH}^{-1}$ for iridium oxide microelectrodes obtained by the Pechini method onto Pt wires [8]. Another possible explanation could be associated with other oxidation states of the material that can produce this variation on slope [24]. Although we do not have a definitive explanation, the present result, as described above, is reproducible and was calculated using triplicate electrodes.

After eight weeks of aging, the sensitivity of the electrode decreases approximately 17% for dry storage, see Fig. 3b. When the material used as disc allow it storage in water. In this sense, storing the sensor in deionized water before a new sequence of experiments is strongly recommended to increase the electrode lifetime as shown by Bezbaruah and Zhang [25].

Finally, a slope change was observed for aged electrodes in the range of $2.5 < \text{pH} < 4.0$ and the second one between $4.0 < \text{pH} < 12.5$. This behavior was observed before by Wipt et al. [26]. The author built a microscopic pH electrodes produced by deposition of hydrous iridium oxide onto carbon fibers. In that work [26], this behavior was attributed to two different mechanisms below and above the pH 6 [27,28]. In the present paper, we believe that this could be related to the aging of the electrode or even with different mechanisms with the transition point around pH 4.

3.3. Test of the RRDE performance for pH measurements under rotation

To determine the average response time, the same titration of Fig. 3a was performed with the RRDE electrode but with some modifications in the data acquisition. The electrode was coupled to a rotation system, and the $E_{\text{IrO}_x, \text{ring}}$ was monitored every 0.1 s. The bulk pH was registered using a combined glass electrode. An acid–base titration was then performed at a rotation rate of 600 rpm and the result is shown in Fig. 4a. With the result displayed in this Figure it is possible to propose that the response time of the electrode is $5.7 \pm 1.0 \text{ s}$, this being the time needed for the potential to stabilize after the addition of an aliquot of titrant. This last value changes during the end points to $7.3 \pm 1.0 \text{ s}$ where the

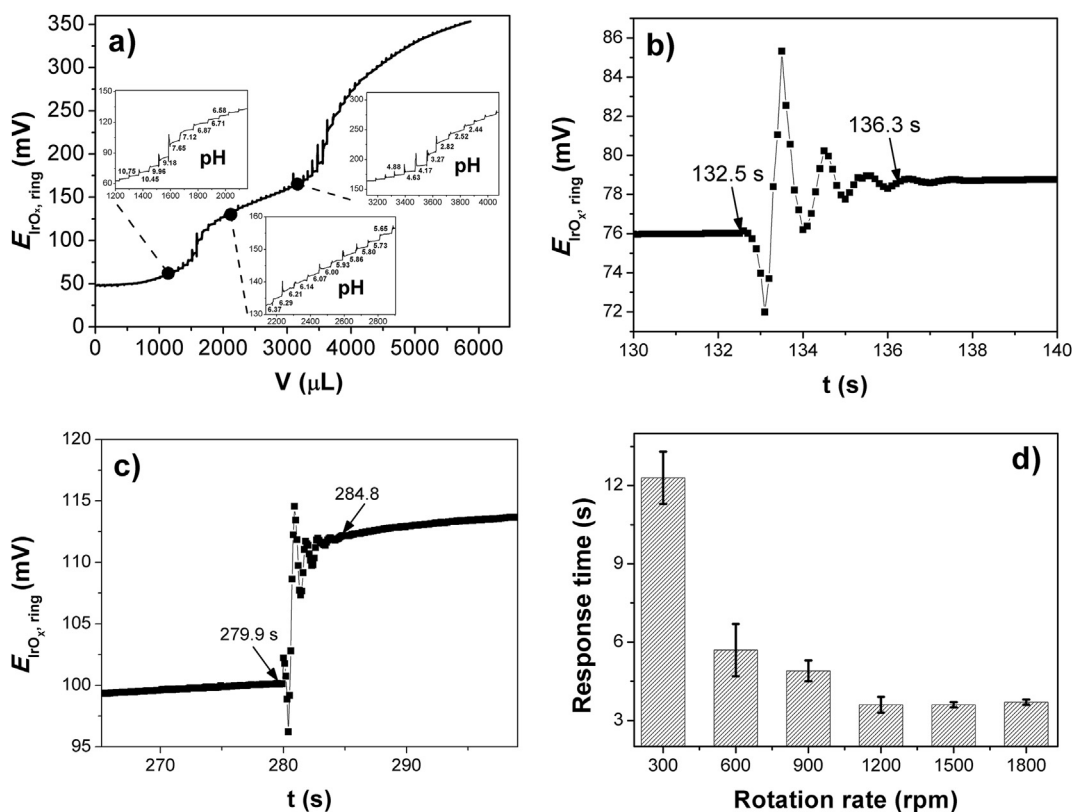


Fig. 4. Titration curve of NaOH (0.1 mol L⁻¹) titrated with H₃PO₄ (1 mol L⁻¹) with the RRDE on rotation of 600 rpm (a). Analysis of transient regions during a titration curve with the RRDE on rotation of 1800 rpm (b) and during the end point at the same rotation rate (c). Average response time until equilibrium when the rotation rate changes: 300, 600, 900, 1200, 1500, and 1800 (d). The $E_{IrOx, ring}$ was collected every 0.1 s during titration. All potential obtained vs. Ag/AgCl/KCl (Sat.).

electrode response was slower. This kind of delay in the stabilization time was also observed in the commercial glass electrode measurements.

For higher rotation rates a different behavior was observed after the addition of an aliquot of titrant. Fig. 4b and c highlight two transient regions for a rotation rate of 1800 rpm between a step potential on the ring during the titration. This kind of transient state was observed for rotation rates over 1500 rpm. The average time for the stabilization of the pH of the solution was 3.7 ± 0.1 s, Fig. 4b, even during the end points, Fig. 4c.

It is also important to stress that the addition of an aliquot of 100 μ L from the acid solution into the alkaline is followed by a fast oscillation of the $E_{IrOx, ring}$ (transient regions) and thereafter by a steady region. Wipf et al. [26] used two time constants to characterize a micro pH electrode. The first is the response time where most of the potential changes occur and the second is the time needed to reach an equilibrium value [26]. The second constant is here defined as an average response time corresponding to the 95% change (t_{95}) of the $E_{IrOx, ring}$ versus time during a pH shift [9]. Such response times were obtained between the two arrows indicated before and after the transient region, as shown in Fig. 4b and c, for a rotation rate of 1800 rpm. In Fig. 4d, the average response time is plotted as a function of the rotating rate, and, as expected, there is a considerable decrease in the response time for rotation rates up to 1200 rpm. Besides, the experimental error also decreases for higher rotation rates. On the other hand, the first constant was also observed here, but with an oscillatory behavior; see the transient region of Fig. 4b and c. This indicates that the RRDE pH sensor built here has a fast first response time, which is an important characteristic for detecting transient pH fluctuations occurring near the surface solution. The initial region of transients occurs within 300–700 ms. After this, a high increment on the $E_{IrOx, ring}$ occurs,

followed by three or four new transients, until the equilibrium is reached. This indicates the high sensitivity of the UME pH sensor even when small pH shifts are taking place on the ring/solution interface, as shown in Fig. 4b and c, where pH shifts of 0.1 and 0.5 pH units were respectively observed (see slopes discussed in the text of Fig. 3b).

3.4. Application of RRDE for interfacial pH measurements under electrochemical polarization on the disc electrode

The water reduction reaction in a solution containing Na₂SO₄ 0.1 mol L⁻¹ (pH 6.5) was used to test the RRDE response when a pH shift is caused by an electrochemical process that produces hydroxyl ions. This solution was degassed for 10 min under N₂, and the $E_{IrOx, ring}$ was monitored under the same conditions. After this step, the solution pH was reduced to approximately 6.0.

Next, the influence of the rotation rate on the steady state was investigated [15] when the ring was used as a potentiometric pH sensor. To achieve these results, the rotation rate was changed from 300 rpm to 1800 rpm during a CA measurement where the potential of -0.5 V was applied for 2100 s. The changes in the rotation rate were performed every 300 s in this experiment and the interfacial pH measured at the ring is shown in Fig. 5.

For this experiment, the slope from the calibration curve of Fig. 3b was used to convert the $E_{IrOx, ring}$ to the pH values found in Fig. 5. It was found that the interfacial pH changes from 8.3 to 7.5 with an increment of the electrode rotation. However, when the rotation rate increases from 1200 to 1800 rpm, the $E_{IrOx, ring}$ only changes from 129.4 ± 5.2 mV to 128.3 ± 0.4 mV. According to this observation, it is possible to affirm that the steady state [15] is achieved at rotation rates over 1200 rpm. This may occur as there is a maximum of efficiency at which species may be thrown from the

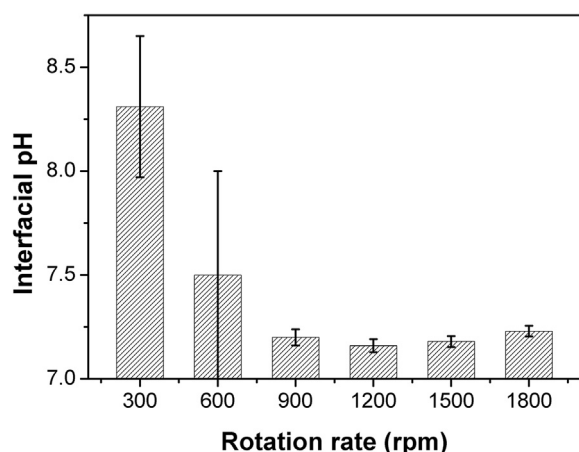


Fig. 5. Interfacial pH measured directly on the ring during a CA experiment at -0.5 V changing the rotation rate: 300, 600, 900, 1200, 1500, and 1800 rpm. Na_2SO_4 0.1 mol L^{-1} solution, pH 6.0.

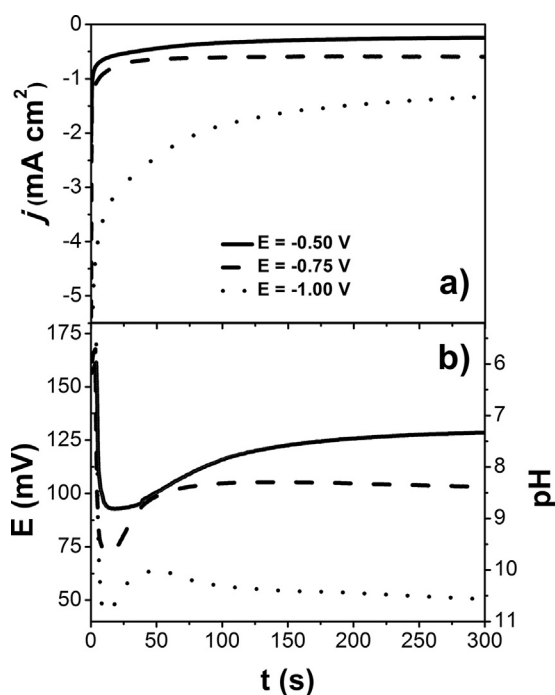


Fig. 6. CA measurements on the copper disc (a) and $E_{\text{IrOx, ring}}$ (b) to different polarization values at -0.5 V (—), -0.75 V (---) and -1.0 V (⋯) in Na_2SO_4 0.1 mol L^{-1} solution, pH 6.0. Rotation rate of 1800 rpm. E vs. $\text{Ag}/\text{AgCl}/\text{KCl}$ (Sat.).

disc to the ring, as observed before in Fig. 4.

The water reduction reaction was investigated at different potentials using the same experimental condition of Fig. 5, but with the RRDE kept on a rotation rate of 1800 rpm. These results are

Table 1
 $E_{\text{IrOx, ring}}$ before, during, and after CA measurements of the disc ($E_{\text{copper, disc}}$) performed at potentials of -0.5 , -0.75 , and -1.0 V at a rotation rate of 1800 rpm together with the interfacial pH obtained from calibration curve of Fig. 3b. E vs. $\text{Ag}/\text{AgCl}/\text{KCl}$ (Sat.).

$E_{\text{copper disc}}/\text{V}$	Rotation rate/rpm	$E_{\text{IrOx ring}} \pm (\text{SE})/\text{mV}$ before the CA	$E_{\text{IrOx ring}} \pm (\text{SE})/\text{mV}$ during the CA	Interfacial pH on the ring	$E_{\text{IrOx ring}} \pm (\text{SE})/\text{mV}$ after the CA
—	1800	157.4 ± 0.6	—	6.0^{a}	—
-0.5	1800	—	126.5 ± 1.5	7.3^{b}	162.3 ± 0.5
-0.75	1800	—	104.2 ± 0.7	8.3^{b}	162.8 ± 0.1
-1.0	1800	—	52.25 ± 1.2	10.6^{b}	166.8 ± 0.6

^a pH measured on bulk solution after being bubbled with N_2 .

^b Interfacial pH based on the slope from calibration curve of Fig. 3b.

shown in Fig. 6. Fig. 6a presents three CAs performed at different potentials on the copper disc at -0.5 V, -0.75 V, and -1.0 V during a period of 300 s, with an interval time of 300 s between each polarization. Fig. 6b shows the $E_{\text{IrOx, ring}}$ during each CA measurement of Fig. 6a. The measurement of the ring potential started 300 s before each cathodic polarization and finished 300 s after it.

The results for the initial condition and for the three experiments are shown in Table 1, where the average ring potential ($\bar{E}_{\text{IrOx, ring}}$) was calculated with its standard error (SE) before and after each step during the last 150 s (Fig. 6b). From this mean value, the interfacial pH was estimated directly on the ring and presented in the penult column of this Table. At the beginning of the measurements the $\bar{E}_{\text{IrOx, ring}}$ was 157.4 ± 0.6 mV. This value was taken as pH 6.0 of the bulk after being bubbled with N_2 . During the CA measurements, a reduction in the $\bar{E}_{\text{IrOx, ring}}$ potential occurs from 126.5 ± 1.5 to 52.25 ± 1.2 . Using the slope from the calibration curve (Fig. 3b), these potential values at the IrOx ring indicate an increase in the interfacial pH from 7.3 (first CA) to 10.6 (third CA), Table 1. The hydrogen ionic activity increment was more than 3 orders of magnitude compared to the first CA and more than 4 orders of magnitude compared to the bulk solution. In other words, during the CA measurements the difference between bulk pH and interfacial were 1.3, 2.3, and 4.6 pH units, respectively. The alkalization of the near surface solution is due to the water reduction over the copper disc where the hydroxyl species were thrown at the IrOx ring by convection caused by the rotation of the RRDE.

The hydroxyl ions produced during the CA measurements lead to a high pH shift near the surface solution but a very small variation in the bulk pH. This statement was confirmed by the observation of the $\bar{E}_{\text{IrOx, ring}}$ after each cathodic polarization in Fig. 6b, where it was observed that the ring potential after each CA measurement (last column) almost returns to its initial value (third column), Table 1.

Finally; it was possible to show that an electrochemical reaction on the disc surface can generate species that change the interfacial pH on electrode/solution interface. Using the RRDE pH sensor with its versatile assembly, it was possible to perform these measurements successfully, indicating an exciting perspective for using this device in future applications.

4. Conclusions

It was shown in this paper how to build a RRDE pH sensor (IrOx/Metal) using the polymeric precursor method (Pechini). In this assembly, many types of substrates as well as those of various geometries and sizes can be employed, giving to this system a great versatility as well as a very low cost of production. The ring thickness of $9.9 \pm 3.7 \mu\text{m}$ was achieved after four applications of the precursor resin onto a glass tube. The number of layers could be increased or reduced to obtain different thicknesses of the IrOx ring for different purposes. The disc could be substituted for any other metallic material or thin film over a metallic substrate when the experimentalist wants to investigate the behavior of the interfacial pH in an electrochemical reaction. Such ability allows the use of the

RRDE pH sensor in corrosion studies, a system that needs a high level of surface preparation, where, for example, the copper of the disc could be substituted by carbon steel.

Even with a low N , 1.9%, due to the low thickness of the ring and the high gap between the disc and the ring, the N_D was 20%, very close to that observed in the literature for commercial systems. The average response time was 3.7 ± 0.1 s even during the end points of the titration measurements, with the RRDE on a rotation rate of 1800 rpm. This result indicates that the RRDE is suitable for measuring transients of pH in the near surface region. However, optimization of the ring gap distance could improve sensor response in future applications.

Finally, the aging of the electrode showed that it is desirable to prepare a new calibration curve before each experiment to verify the ring response from pH changes after a long storage time.

Acknowledgment

The authors would like to thank FAPESP (Proc. 2013/13503-0, 2011/19430-0, Grants #2013/07296-2, #2012/07313-1, #2013/16930-7), CNPq (Grant # 304458/2013-9), and CAPES for financial support.

References

- [1] J.S. Santos, F. Trivinho-Strixino, E.C. Pereira, Investigation of $\text{Co}(\text{OH})_2$ formation during cobalt electrodeposition using a chemometric procedure, *Surf. Coat. Tech.* 205 (2010) 2585–2589.
- [2] J.S. Santos, R. Matos, F. Trivinho-Strixino, E.C. Pereira, Effect of temperature on Co electrodeposition in the presence of boric acid, *Electrochim. Acta* 53 (2007) 644–649.
- [3] A.M. Zimer, E.C. Rios, P.C.D. Mendes, W.N. Gonçalves, O.M. Bruno, E.C. Pereira, L.H. Mascaro, Investigation of AISI 1040 steel corrosion in H_2S solution containing chloride ions by digital image processing coupled with electrochemical techniques, *Corros. Sci.* 53 (2011) 3193–3201.
- [4] M. Nobial, O. Devos, O. Rosa, B. Tribollet, The nitrate reduction process: a way for increasing interfacial pH, *J. Electroanal. Chem.* 600 (2007) 87–94.
- [5] A. Brenner, *Electrodeposition of Alloys. Principles and Practice*, Academic Press, New York, 1963.
- [6] H. Nakano, M. Matsuno, S. Oue, M. Yano, S. Kobayashi, H. Fukushima, Mechanism of anomalous type electrodeposition of Fe-Ni alloys from sulfate solutions, *Mater. Trans.* 45 (2004) 3130–3135.
- [7] C. Deslouis, I. Frateur, G. Maurin, B. Tribollet, Interfacial pH measurement during the reduction of dissolved oxygen in a submerged impinging jet cell, *J. Appl. Electrochem.* 27 (1997) 482–492.
- [8] A.M. Zimer, S.G. Lemos, L.A. Pocrifka, L.H. Mascaro, E.C. Pereira, Needle-like IrO_2/Ag combined pH microelectrode, *Electrochem. Commun.* 12 (2010) 1703–1705.
- [9] I.A. Ges, B.L. Ivanov, D.K. Schaffer, E.A. Lima, A.A. Werdich, F.J. Baudenbacher, Thin-film IrOx pH microelectrode for microfluidic-based microsystems, *Biosens. Bioelectron.* 21 (2005) 248–256.
- [10] R. Bashir, J.Z. Hilt, O. Elibol, A. Gupta, N.A. Peppas, Micromechanical cantilever as an ultrasensitive pH microsensor, *Appl. Phys. Lett.* 81 (2002) 3091–3093.
- [11] J. Li, Y. Du, C. Fang, Developing an iridium oxide film modified microelectrode for microscale measurement of pH, *Electroanal. Chem.* 608–611.
- [12] X. Zhang, H. Ju, J. Wang, *Electrochemical Sensors, Biosensors and Their Biomedical Applications*, first ed., Elsevier Inc., New York, 2008.
- [13] W.J. Albery, E.J. Calvo, Ring-disc electrodes part 21. – pH measurement with the ring, *J. Chem. Soc. Faraday Trans. 1* (79) (1983) 2583–2596.
- [14] P. Steegstra, E. Ahlberg, In situ pH measurements with hydrous iridium oxide in a rotating ring disc configuration, *J. Electroanal. Chem.* 685 (2012) 1–7.
- [15] A.J. Bard, L.R. Faulkner, *Electrochemical Methods Fundamentals and Applications*, second ed., John Wiley & Sons, Inc., New York, 2010.
- [16] S. Vesztegom, M. Ujvári, G.G. Láng, RRDE experiments with potential scans at the ring and disk electrodes, *Electrochem. Commun.* 13 (2011) 378–381.
- [17] W.J. Albery, S. Bruckenstein, Ring-disc electrodes part 2. – theoretical and experimental collection efficiencies, *Trans. Faraday Soc.* 62 (1966) 1920–1931.
- [18] A. Fog, R.P. Buck, Electronic semiconducting oxides as pH sensor, *Sens. Actuat. B* 5 (1984) 137–146.
- [19] L.A. Pocrifka, C. Gonçalves, P. Grossi, P.C. Colpa, E.C. Pereira, Development of $\text{RuO}_2\text{-TiO}_2$ (70–30) mol% for pH measurements, *Sens. Actuat. B* 113 (2006) 1012–1016.
- [20] S. Ardizzone, A. Carugati, S. Trasatti, Properties of thermally prepared iridium dioxide electrodes, *J. Electroanal. Chem.* 126 (1981) 287–292.
- [21] M.A. Petit, V. Plichon, Anodic electrodeposition of iridium oxide films, *J. Electroanal. Chem.* 444 (1998) 247–252.
- [22] J.J. Miksis Jr., J. Newman, Primary resistances for ring-disk electrodes, *J. Electrochem. Soc.* 123 (1976) 1030–1036.
- [23] C.M.A. Brett, A.M.O. Brett, *Electrochemistry: Principles, Methods, and Applications*, first ed., Oxford, New York, 1993.
- [24] M. Pourbaix, *Atlas of Electrochemical Equilibria in Aqueous Solution*, second ed., NACE International, Houston, 1974.
- [25] A.N. Bezbaruah, T.C. Zhang, Fabrication of anodically electrodeposited iridium oxide film pH microelectrodes for microenvironmental studies, *Anal. Chem.* 74 (2002) 5726–5733.
- [26] D.O. Wipf, F. Ge, T.W. Spaine, J.E. Baur, Microscopic measurement of pH with iridium oxide microelectrodes, *Anal. Chem.* 72 (2000) 4921–4927.
- [27] P.G. Pickup, V.I. Birss, A model for anodic hydrous oxide growth at iridium, *J. Electroanal. Chem.* 220 (1987) 83–100.
- [28] R.K. Jaworski, J.A. Cox, B.R. Strohmeier, Characterization of oxide films electrochemically deposited from solutions of palladium chloride and sodium hexachloroiridate, *J. Electroanal. Chem.* 325 (1992) 111–123.